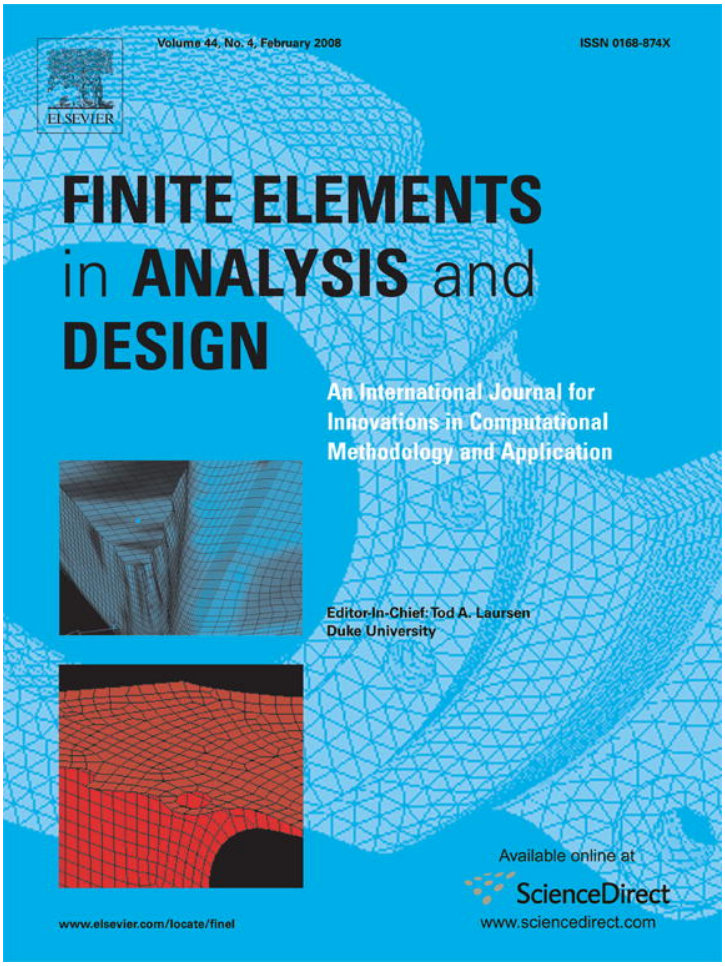

Available online at www.sciencedirect.com
ScienceDirect
Finite Elements in Analysis and Design 44 (2008) 214–224
FINITE ELEMENTS IN ANALYSIS AND DESIGN
www.elsevier.com/locate/finel

Analysis of moving loads using force-based finite elements

Adrian Kidarsa[a], Michael H. Scott[b,*], Christopher C. Higgins[b]

[a]*T.Y. Lin International, Salem, OR 97302, USA*
[b]*School of Civil and Construction Engineering, Oregon State University, Corvallis, OR 97331, USA*

Received 12 May 2007; received in revised form 17 October 2007; accepted 27 November 2007
Available online 7 January 2008

Abstract

An analysis method for moving loads computes the internal force history in a structural member at the integration points of force-based finite elements as opposed to the end forces of a refined displacement-based finite element mesh. The force-based formulation satisfies strong equilibrium of internal section forces with the element end forces and the moving load. This is in contrast with displacement-based finite element formulations that violate equilibrium between the section forces and the equivalent end forces computed for the moving load. A new approach to numerical quadrature in force-based elements allows the specification of integration point locations where the section demand is critical while ensuring a sufficient level of integration accuracy over the element domain. Influence lines computed by numerical integration in force-based elements converge to the exact solution and accurate results are obtained for practical applications in structural engineering through the new low-order integration approach. The proposed methodology for moving load analysis has been incorporated in automated software to load rate a large number of bridges efficiently.

Keywords: Finite elements; Influence lines; Load rating; Moving loads; Numerical integration; Simulation models; Structural analysis

1. Introduction

Moving load analysis requires an accurate computation of structural response quantities in order to determine the position or combination of live loads that will produce the highest demand at critical locations in a structure. Examples of critical locations are flexural bar cutoffs or changes in stirrup spacing in reinforced concrete members and section transitions in built-up steel members. Influence lines show the variation of a particular response quantity (shear force, bending moment, etc.) at a location as a unit load moves across the structure. An influence line can then be used to evaluate the magnitude of the response quantity for more complex loading events. Influence lines are particularly useful for the analysis of vehicle loads on bridge structures, loads on crane runways, and live load patterns in multi-story frame structures.

Qualitative influence lines can be constructed using the Müller–Breslau principle described in structural analysis texts; however, it is often necessary to generate quantitative influence lines for structural design and assessment. Classical structural analysis methods, such as moment distribution and slope-deflection, become relatively time consuming when used to construct quantitative influence lines. Computerized structural analysis programs provide a more efficient alternative by allowing repeated analyses for several positions of a moving load.

The most common approach to compute internal forces is to use displacement-based finite elements, which prescribe an approximate displacement field along the element [1–3]. The displacement fields for standard beam-column finite element implementations, e.g., assumed linear axial displacement and cubic Hermitian transverse displacement fields, do not account for interior element loads, such as a point load that moves across the element domain. Consistent with the principle of virtual displacements, the computation of equivalent end forces for the finite element solution produces a weak equilibrium error between the element end forces, the moving load, and the internal section forces along the element. This error is mitigated

* Corresponding author. Tel.: +1 541 737 6996; fax: +1 541 737 3052.
E-mail addresses: akidarsa@tylin.com (A. Kidarsa), michael.scott@oregonstate.edu (M.H. Scott), chris.higgins@oregonstate.edu (C.C. Higgins).

0168-874X/$ - see front matter © 2007 Elsevier B.V. All rights reserved.
doi:10.1016/j.finel.2007.11.013

Nomenclature

b section force interpolation matrix
e section deformation vector
$\mathbf{f}_s$ section flexibility matrix
$\mathbf{k}_s$ section stiffness matrix
N number of element integration points
q element basic force vector
s section force vector
$\mathbf{s}_p$ section force vector due to interior element loads
v element deformation vector
w integration point weight
x integration point location

by placing a node at each critical location along the member (h-refinement) and treating the internal forces of the member as the end forces of the elements in the refined mesh. The drawback to this rigid body equilibrium calculation is that it decouples the internal member forces from a constitutive relationship that accounts for interaction, e.g., moment and shear, at the critical location. Timoshenko beam elements account for moment–shear interaction along the element length, but this approach still suffers from the aforementioned error in weak equilibrium in the presence of interior loads and thus requires refinement of the finite element mesh.

An alternative approach to simulate beam-column response is the force-based formulation [4], which imposes strong equilibrium of internal section forces with the element end forces and loads applied on the element interior. This equilibrium condition alleviates the need for mesh refinement in order to compute the internal forces in a structural member subjected to a moving load. The internal forces are computed at the integration points of the finite element and only a numerical integration error is present in the analysis. The drawback to the force-based approach, however, is the integration point locations seldom coincide with critical locations along the structural member. As a result, it is difficult to compute the internal section forces at specified critical locations when using force-based elements to simulate the response of a structure to moving loads. Neuenhofer and Filippou [5] give details on how force-based elements are implemented in a general stiffness-based finite element setting and describe the advantages of using force-based elements to simulate nonlinear material response.

This paper explores additional advantages of force-based elements in analyzing planar structures for moving loads. A new approach to numerical integration in force-based finite elements, where the specification of critical section locations as the element integration points makes mesh refinement unnecessary, is also developed. These objectives are addressed by performing static, two-dimensional analyses of moving loads, the results of which can be modified by impact and distribution factors in order to approximate dynamic effects of vehicle loading and three-dimensional effects of load transfer, e.g., through a bridge deck. This modeling approach reflects the state of practice in the design and load rating of bridge girders. State of the art finite element models that account explicitly for vehicle–bridge dynamic interaction have been developed by several researchers, e.g., Tan et al. [6], Ju et al. [7], and Kwasniewski et al. [8] to name a few, but are not addressed herein.

This paper begins with an overview of the force-based element formulation, along with a comparison of the internal equilibrium conditions that arise in displacement- and force-based elements due to a point load that moves along a simply supported structural member. Optimal quadrature methods that have a high order of integration accuracy are summarized next, followed by the development of the new low-order integration approach that allows the location of each integration point to be specified along with the associated integration weights at a selected number of points. The remaining integration weights are computed in order to ensure numerical integration accuracy over the entire element domain. This paper concludes with example applications that demonstrate the numerical accuracy of the new integration approach in force-based elements is on par with that offered by optimal quadrature rules, but with the important advantage of computing the internal force history at user-defined critical locations along a structural member during a moving load analysis.

2. Force-based finite element formulation

The force-based beam elements considered in this paper are formulated in a two-dimensional basic system, free of rigid body displacement modes [9]. The simply supported basic system is shown in Fig. 1, where the basic forces (axial force and end moments) are collected in the vector

$$\mathbf{q} = [\, q_1 \quad q_2 \quad q_3 \,]^{\mathrm{T}}. \tag{1}$$

The corresponding element deformations are the change in length and the end rotations

$$\mathbf{v} = [\, v_1 \quad v_2 \quad v_3 \,]^{\mathrm{T}}. \tag{2}$$

The internal forces at any location, x, along the element are collected in the section force vector

$$\mathbf{s}(x) = [\, P(x) \quad M(x) \quad V(x) \,]^{\mathrm{T}}, \tag{3}$$

where P is the section axial force, M is the section bending moment, and V is the section shear force (Fig. 1). The corresponding section deformations, or section strains, are collected in the vector

$$\mathbf{e}(x) = [\, \varepsilon(x) \quad \kappa(x) \quad \gamma(x) \,]^{\mathrm{T}}, \tag{4}$$

where ε is the axial deformation, κ is the curvature, and γ is the shear deformation of the section, each of which is

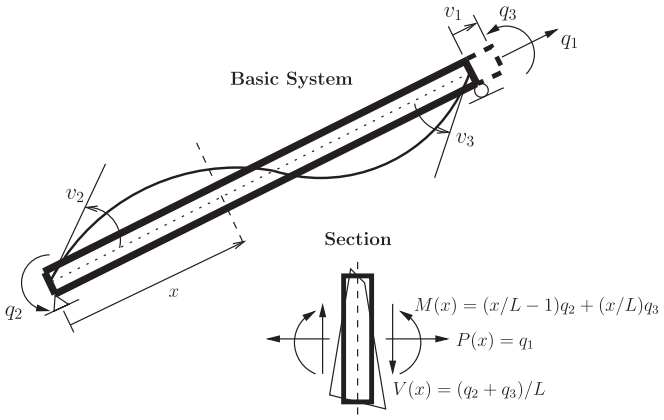

Fig. 1. Simply supported basic system and section forces for two-dimensional beam-column elements.

work-conjugate to the corresponding value in $\mathbf{s}(x)$. Equilibrium between section forces and the basic forces and applied element loads is expressed in strong form:

$$\mathbf{s}(x) = \mathbf{b}(x)\mathbf{q} + \mathbf{s}_{\mathrm{p}}(x). \tag{5}$$

The matrix $\mathbf{b}(x)$ contains the force interpolation functions that represent the homogeneous solution to beam equilibrium (constant axial and shear forces with linearly varying bending moment):

$$\mathbf{b}(x) = \begin{bmatrix} 1 & 0 & 0 \\ 0 & x/L - 1 & x/L \\ 0 & 1/L & 1/L \end{bmatrix}. \tag{6}$$

The vector $\mathbf{s}_{\mathrm{p}}(x)$ in Eq. (5) represents the particular solution to beam equilibrium for an interior element load applied in the basic system. Expressions for $\mathbf{s}_{\mathrm{p}}(x)$ considering several types of element loading are found in structural analysis texts. For a transverse point load, F, located a distance x_0 along an element, this vector is

$$\mathbf{s}_{\mathrm{p}}(x) = \begin{bmatrix} 0 \\ FL\xi_0(1-\xi_0)(1-(\xi_0-\xi)/\xi^*) \\ F\xi_0(1-\xi_0)/\xi^* \end{bmatrix}, \tag{7}$$

where $\xi = x/L$ and $\xi_0 = x_0/L$, as shown in Fig. 2, and

$$\xi^* = \begin{cases} \xi_0, & \xi \leqslant \xi_0, \\ \xi_0 - 1, & \xi > \xi_0. \end{cases} \tag{8}$$

For a transverse load that moves across the element, the section forces in Eq. (7) evolve as a function of the position variable ξ_0. An important advantage of the force-based formulation is the ability to account for section shear force directly in the element equilibrium relationship [10]. For moving load analysis, the section shear force is computed from static equilibrium of the basic forces and the interior point load applied at a given location.

The section forces are related to the section deformations through a constitutive relationship. In this paper, linear-elastic

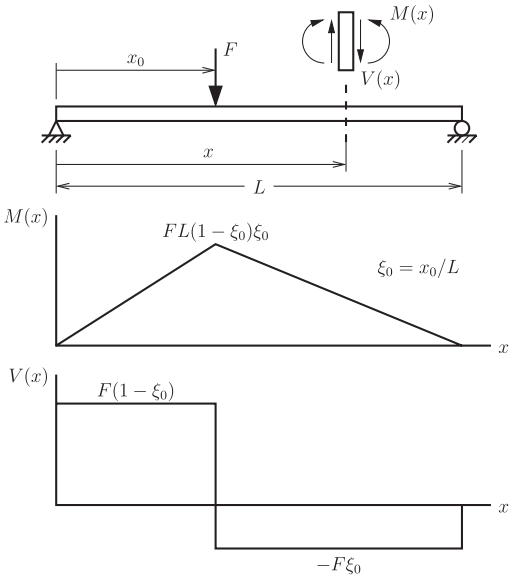

Fig. 2. Bending moment and shear force developed in the simply supported basic system for a transverse point load.

section response is considered, where the section forces are expressed as a matrix–vector product of the section deformations:

$$\mathbf{s}(x) = \mathbf{k}_{\mathrm{s}}(x)\mathbf{e}(x), \tag{9}$$

where $\mathbf{k}_{\mathrm{s}}$ is the matrix of section stiffness coefficients derived from the material properties and dimensions of the cross-section. In the force-based formulation, it is necessary to express the section force–deformation relationship of Eq. (9) in compliance form:

$$\mathbf{e}(x) = \mathbf{f}_{\mathrm{s}}(x)\mathbf{s}(x), \tag{10}$$

where $\mathbf{f}_{\mathrm{s}}(x) = \mathbf{k}_{\mathrm{s}}^{-1}(x)$ is the section flexibility matrix.

According to the principle of virtual forces, along with Eqs. (5) and (10), the element compatibility relationship in the force-based formulation is expressed in integral form:

$$\mathbf{v} = \left(\int_0^L \mathbf{b}^{\mathrm{T}}(x)\mathbf{f}_{\mathrm{s}}(x)\mathbf{b}(x)\,\mathrm{d}x \right)\mathbf{q} + \int_0^L \mathbf{b}^{\mathrm{T}}(x)\mathbf{f}_{\mathrm{s}}(x)\mathbf{s}_{\mathrm{p}}(x)\,\mathrm{d}x. \tag{11}$$

It is assumed in this paper that Eq. (11) is evaluated by an N-point numerical integration rule as a summation of N discrete function evaluations at locations, $x_1, \ldots, x_N$, with associated integration weights, $w_1, \ldots, w_N$:

$$\mathbf{v} = \left(\sum_{i=1}^{N} \mathbf{b}^{\mathrm{T}}(x_i)\mathbf{f}_{\mathrm{s}}(x_i)\mathbf{b}(x_i)w_i \right)\mathbf{q} + \sum_{i=1}^{N} \mathbf{b}^{\mathrm{T}}(x_i)\mathbf{f}_{\mathrm{s}}(x_i)\mathbf{s}_{\mathrm{p}}(x_i)w_i. \tag{12}$$

For a prismatic element, $\mathbf{f}_{\mathrm{s}}(x)$ is constant along the length, and quadratic polynomials appear in the first term on the right-hand side of Eq. (12) from the squaring of the linear interpolation functions in $\mathbf{b}(x)$, thus it is possible to evaluate this term exactly with a quadrature rule that exactly integrates quadratic

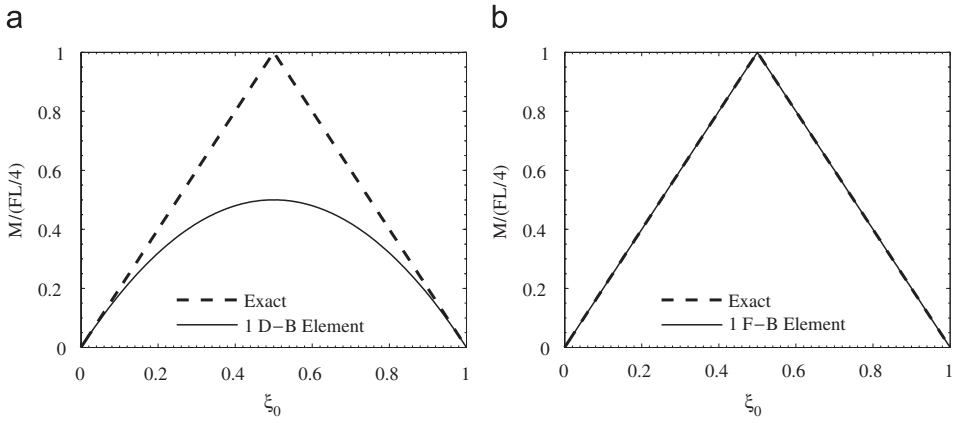

Fig. 3. Comparison of the computed and exact solutions to the influence line for the midspan bending moment of a simply supported beam using: (a) a single displacement-based element; (b) a single force-based element.

polynomials. The second term on the right-hand side of Eq. (12) contains a discontinuity in $\mathbf{s}_p(x)$ when a transverse point load is applied on the element interior, which is evident from the jump in the shear diagram of Fig. 2. Consistent with numerical analysis theory, an error will appear from evaluating this term by numerical integration because the stated accuracy of any quadrature method is based on the assumption of continuity, of the integrand and its derivatives [11].

With the overview of the force-based formulation complete, the difference between the displacement- and force-based formulations is illustrated in the moving load analysis of the simply supported beam shown in Fig. 2. The analysis is performed with a single displacement-based element (cubic Hermitian polynomials for the transverse displacement field), and then the analysis is repeated using a single force-based element. The governing equations in each element formulation are evaluated by three-point Gauss–Lobatto quadrature in order to compute an influence line for the midspan bending moment. As seen in Fig. 3, there is a significant error in the influence line computed with one displacement-based element since the internal bending moment is constrained to the equivalent end moments computed from the transverse displacement field. On the other hand, the analysis with one force-based element captures the exact solution. There is no numerical integration error in the force-based solution because the structure is statically determinate, i.e., no compatibility equations have to be satisfied by the analysis. The exact solution for the midspan moment influence line in the displacement-based formulation can be obtained by subdividing the span into two elements with an additional node at midspan. The midspan moment is then equal to the end moments of the adjacent elements; however, this approach is less than ideal because it requires refinement of the finite element mesh and it decouples the internal force computation from a constitutive model that accounts for the interaction of section forces at the element integration points.

3. Optimal element integration methods

This section contains an overview of two optimal numerical integration methods that integrate the highest order polynomial possible under the given constraints on the integration point locations and weights. First is Gauss–Lobatto quadrature, which is commonly used in the implementation of force-based finite elements. This is followed by the method of undetermined coefficients, of which Newton–Cotes quadrature is a special case.

3.1. Gauss–Lobatto quadrature

Gauss–Lobatto quadrature [12] is the standard approach to evaluate the element integral (Eq. (12)) in the force-based formulation because it places sample points at the element ends, where bending moments are largest in the absence of interior element loads. This quadrature method exactly integrates polynomials up to order $2N-3$, i.e., from x^0 to x^{2N-3}, where N is the number of sample points. In addition to its high order of accuracy, Gauss–Lobatto quadrature is numerically stable since all integration weights are positive for any selection of N. The primary disadvantage to this approach is the locations and weights of the sample points are determined from optimality conditions for the integration of high-order polynomials that are rarely encountered in practical structural engineering applications. Accordingly, neither the locations nor the weights of the sample points (excluding those at the element ends) have any correlation to the physical characteristics of a structural system, e.g., the location of bar cut-offs, changes in stirrup spacing, or observed plastic hinge lengths [13]. Furthermore, the high order of integration accuracy for this quadrature method in the force-based formulation is compromised because discontinuities appear in the integrand of Eq. (12) in the presence of interior point loads.

3.2. Method of undetermined coefficients

To alleviate the optimality constraints imposed by the Gauss–Lobatto quadrature method, it is possible to specify the location of each sample point and construct a quadrature method of a lower order of integration accuracy. This approach treats the N sample point locations, $x_1, \ldots, x_N$, as known values while the associated weights, $w_1, \ldots, w_N$, are computed

in order to ensure exact integration of polynomials up to order $N-1$. The integration weights are found by the solution for the undetermined coefficients in the Vandermonde system [14]:

$$\begin{bmatrix} 1 & 1 & \cdots & 1 \\ x_1 & x_2 & \cdots & x_N \\ \vdots & \vdots & \ddots & \vdots \\ x_1^{N-1} & x_2^{N-1} & \cdots & x_N^{N-1} \end{bmatrix} \cdot \begin{bmatrix} w_1 \\ w_2 \\ \vdots \\ w_N \end{bmatrix} = \begin{bmatrix} b-a \\ (b^2-a^2)/2 \\ \vdots \\ (b^N-a^N)/N \end{bmatrix}, \tag{13}$$

where $[a, b]$ is the interval of integration. Although this approach to constructing a quadrature rule permits complete control over the location of sample points in a force-based element, there is no control over the resulting integration weights. In fact, this approach is generally unstable because negative integration weights can appear for any $N \geqslant 2$, i.e., the sum of the absolute values of the integration weights is greater than the length of the integration domain. Negative integration weights can lead to a non-unique solution where the computed response can change significantly as a function of the number and location of sample points. It is noted that the solution of the Vandermonde system in Eq. (13) for equally spaced sample point locations generates the Newton–Cotes quadrature method [12], which is stable for any $N < 9$.

4. Low-order approach to undetermined coefficients

As discussed in the previous section, neither Gauss–Lobatto quadrature nor the method of undetermined coefficients permits complete control over the location and weight of each sample point. Furthermore, negative integration weights can appear via the method of undetermined coefficients by forcing the resulting quadrature rule to represent polynomials up to order $N-1$, thereby leading to numerical instability and non-uniqueness of the computed solution.

In this section, an alternative approach is taken to the method of undetermined coefficients to construct an N-point quadrature rule with specified point locations. This approach is based on the following observations:

1. There will be a numerical integration error for any quadrature method that is used to evaluate the force-based element compatibility relationship when a transverse point load is applied on the element interior and causes a discontinuity of the integrand in Eq. (12).
2. For the common case of a prismatic element without interior loads ($\mathbf{s}_p(x) = \mathbf{0}$), the integration of quadratic polynomials is sufficient to represent the product of a linear curvature distribution with the linear bending moment interpolation functions in Eq. (12).

From these observations, it is seen that for an N-point quadrature rule with specified locations, only three integration weights need to be treated as unknown in order to integrate up to quadratic polynomials, i.e., x^0, x^1, and x^2, which are necessary to represent a linear curvature distribution along an element. As a result, the remaining $N-3$ weights can be specified in addition to the N locations while maintaining a sufficient level of numerical accuracy for elements without interior point loads.

To formalize this procedure of constructing an N-point quadrature rule with specified locations and partially specified weights, the integration points are divided into two groups, those constrained to have a specified weight and those where the weight is treated as unknown. The number of integration points where the corresponding weight is specified is N_c, while $N_f = N - N_c$ is the number of integration points where the associated weight is unknown. Accordingly, the integration point locations are denoted x_f and x_c, while the weights are w_f and w_c. A Vandermonde system on the order of N_f can then be solved to obtain the unknown weights, which will ensure accurate integration of polynomials up to the order of $N_f - 1$. Consequently, Eq. (13) is modified by moving to the right-hand side the contributions of the N_c integration points for which both the location and weight are specified

$$\begin{bmatrix} 1 & 1 & \cdots & 1 \\ x_{f1} & x_{f2} & \cdots & x_{fN_f} \\ \vdots & \vdots & \ddots & \vdots \\ x_{f1}^{N_f-1} & x_{f2}^{N_f-1} & \cdots & x_{fN_f}^{N_f-1} \end{bmatrix} \cdot \begin{bmatrix} w_{f1} \\ w_{f2} \\ \vdots \\ w_{fN_f} \end{bmatrix} = \begin{bmatrix} (b-a) - \sum_{j=1}^{N_c} w_{cj} \\ (b^2-a^2)/2 - \sum_{j=1}^{N_c} x_{cj} w_{cj} \\ \vdots \\ (b^{N_f}-a^{N_f})/N_f - \sum_{j=1}^{N_c} x_{cj}^{N_f-1} w_{cj} \end{bmatrix}. \tag{14}$$

To ensure that the integration rule can represent a linear curvature distribution, which occurs in the analysis of prismatic structural members without interior loads, $N_f \geqslant 3$ is required. Although this approach does not guarantee that all integration weights computed via Eq. (14) will be positive, it makes the resulting quadrature rule physically significant by allowing the integration weights to be specified at selected locations and removes the constraints of integrating high-order polynomials that are rarely encountered in structural engineering applications. Thus, in addition to moving load analysis, this numerical integration approach is suited to represent nonlinear material response over prescribed lengths in a structural member, e.g., in plastic hinge zones of beam-column members and in shear critical D-regions adjacent to continuous beam supports.

5. Numerical examples

The low-order approach to the method of undetermined coefficients presented in this paper has been implemented in the OpenSees finite element software framework [15] to complement the existing implementation of force-based elements using Gauss–Lobatto integration. The convergence behavior of each approach to numerical integration in the force-based

formulation is investigated for computing influence lines in the first example. Then, applications to the moving load analysis of a bridge structure are explored in the second example.

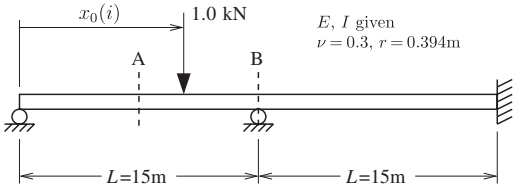

Fig. 4. Two-span structure with a single force-based element along each span and internal forces computed at section A (middle of span 1) and section B (end of span 1) for a moving unit load.

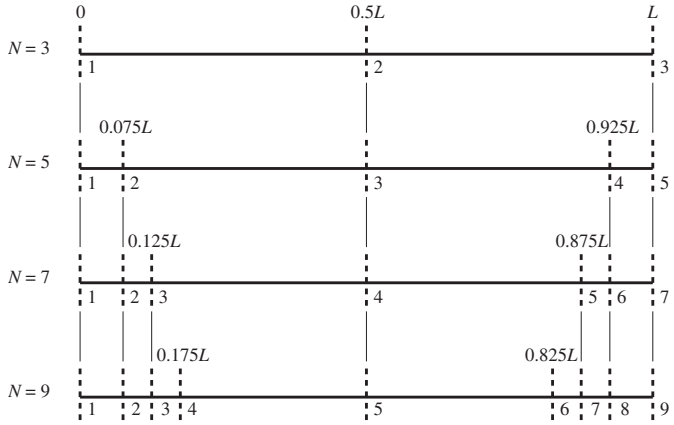

Fig. 5. Integration point locations used in the undetermined coefficients and low-order undetermined coefficients approaches to demonstrate the convergence behavior of the moment and shear influence lines computed using a single force-based element in each span of the two-span structure in Fig. 4.

5.1. Convergence of influence lines for each quadrature method

In this example, moment and shear influence lines computed by the integration methods presented in this paper are compared to the exact solution for the bending moment and shear forces developed at sections A and B in the two-span structure shown in Fig. 4. Section A is at the middle of span 1, a location of high moment and low shear; whereas section B is located at the right end of span 1, just to the left of the continuous support, at a negative moment location with high shear. The structure has a prismatic cross-section and linear-elastic material properties for flexural and shear deformations at each section. Poisson's ratio is assumed to be 0.3 and the radius of gyration for the cross-section is 0.394 m. Each span length is $L = 15$ m.

The convergence of the computed influence lines is demonstrated using a single force-based finite element per span with $N = 3$, 5, 7, and 9 integration points in each quadrature method. An odd number of integration points in the Gauss–Lobatto and Newton–Cotes methods will ensure that internal forces will be sampled at sections A and B of the structure. For the quadrature approaches based on undetermined coefficients, integration points are placed at the middle and at the ends of each element with successive integration points placed on the interior of the domain for $N > 3$. For the low-order approach, the weights at the middle three integration points are treated as undetermined coefficients, while the weights at the remaining $N - 3$ integration points are set equal to $0.05L$. These integration point locations are shown in Fig. 5, and the associated integration weights computed by Eqs. (13) and (14) for each approach are listed in Table 1.

Table 1
Integration weights computed by undetermined coefficients and the low-order approach to undetermined coefficients in order to investigate the convergence behavior of each quadrature method

				Undetermined coefficients	Low-order
	i	x_i/L, $1.0 - x_{N-i+1}/L$		w_i, $w_{N-i+1}(/L)$	w_i, w_{N-i+1} $(/L)$
$N = 3$	1	0.0		0.1667	0.1667
	2	0.5		0.6667	0.6667
			$\sum \lvert w_i \rvert / L$	1.0	1.0
$N = 5$	1	0.0		−0.07357	0.05
	2	0.075		0.3325	0.1615
	3	0.5		0.4821	0.5770
			$\sum \lvert w_i \rvert / L$	1.294	1.0
$N = 7$	1	0.0		0.08781	0.05
	2	0.075		−0.2783	0.05
	3	0.125		0.4977	0.1432
	4	0.5		0.3857	0.5136
			$\sum \lvert w_i \rvert / L$	2.113	1.0
$N = 9$	1	0.0		−0.001350	0.05
	2	0.075		0.3714	0.05
	3	0.125		−0.6366	0.05
	4	0.175		0.6101	0.1241
	5	0.5		0.3219	0.4519
			$\sum \lvert w_i \rvert / L$	3.561	1.0

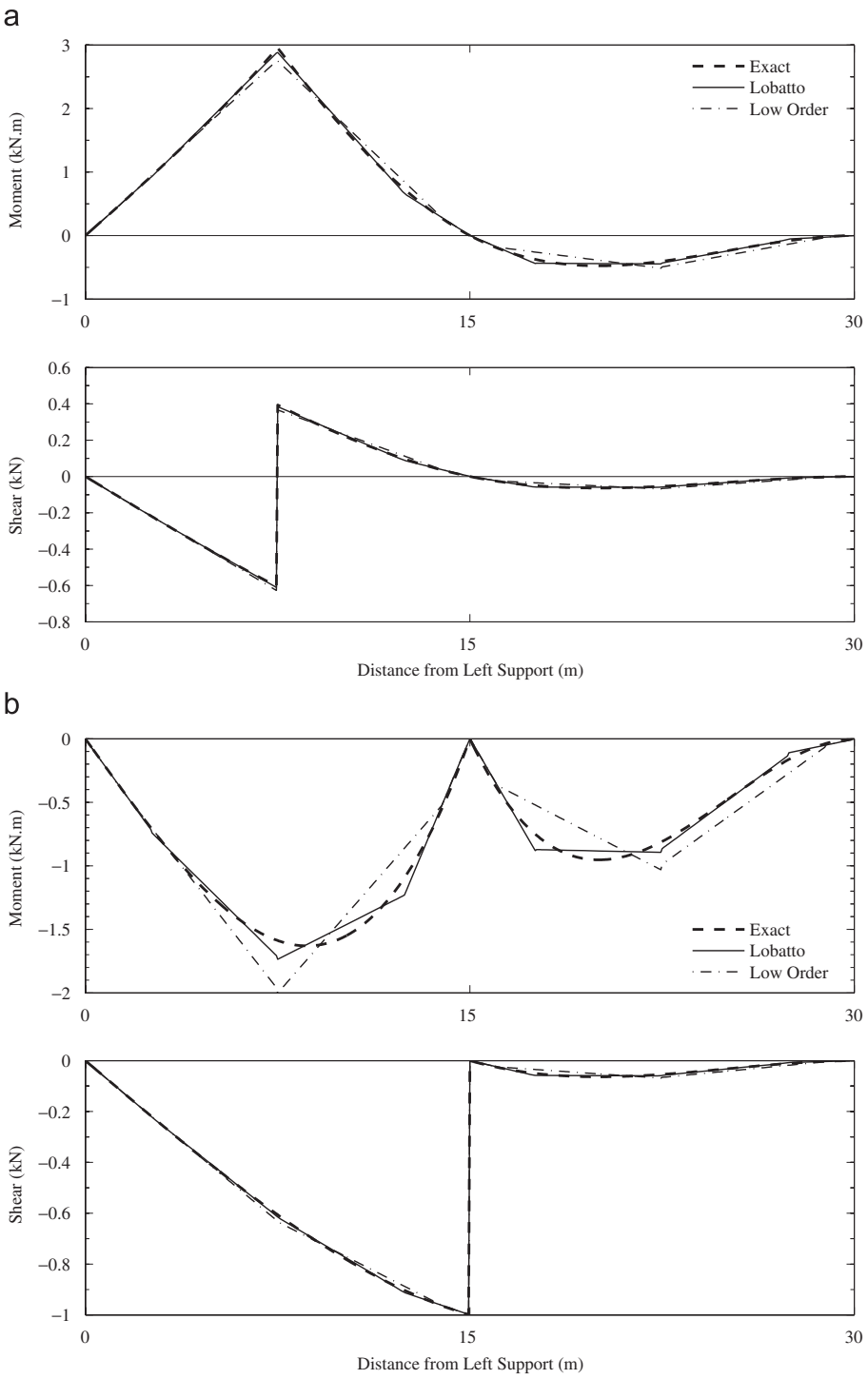

Fig. 6. Moment and shear influence lines for the two-span structure of Fig. 4 computed with the five point ($N=5$) Gauss–Lobatto and low-order undetermined coefficients approaches: (a) middle of span 1; (b) right end of span 1.

The results of the moving load analysis using the Gauss–Lobatto and the low-order undetermined coefficients integration methods with $N=5$ are shown in Fig. 6 as influence lines for the internal moment and shear at sections A and B of the two-span structure. As seen in Fig. 6(a), the computed solution matches the exact solution for the moment and shear influence lines at section A, where flexural response dominates. At section B, with negative moment and high shear, there is a noticeable error in the computed solution for the moment influence line shown in Fig. 6(b). This error is significant in both the Gauss–Lobatto and the low-order integration approaches, and it arises from the change in sign of the section shear force interpolated from the moving load as the load moves across each integration point. As seen in the shear diagram of Fig. 2, when the load is just

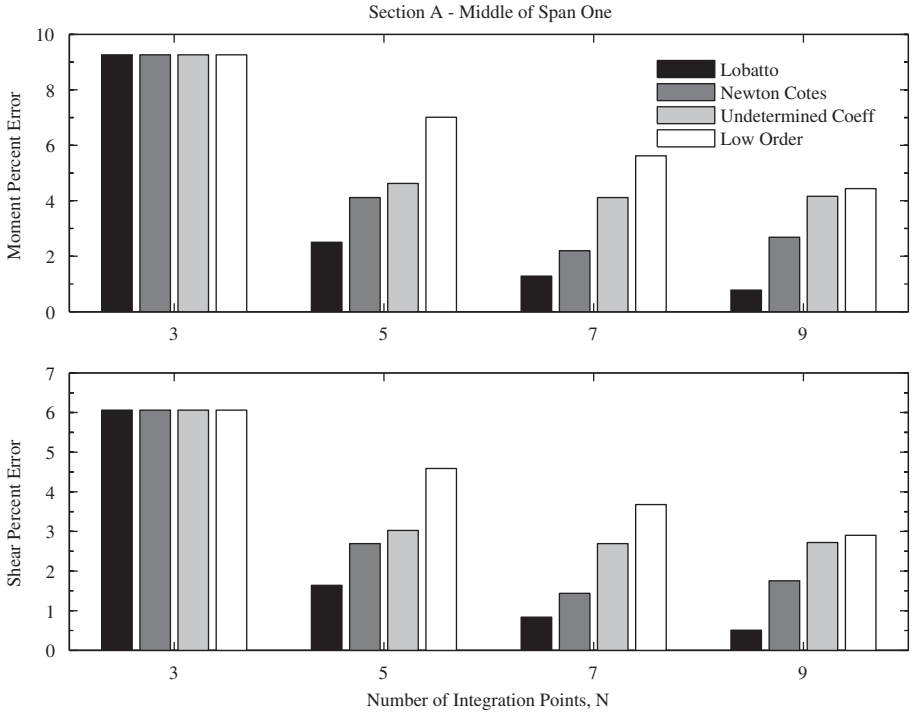

Fig. 7. Percent errors for the internal moment and shear computed at section A of the two-span structure in Fig. 4 for each numerical integration approach with an increasing number of integration points.

to the left of a particular section, the section shear force is positive. Then the load moves just to the right of the section and the shear force suddenly changes to a negative value. These errors are more significant at the shear critical section B than at section A because the effect of shear deformation on the element compatibility relationship is negligible at midspan. It is noted that numerical errors occur at the critical sections in the first span even as the load moves across the second span because the numerical error of the element compatibility relationship in the second span will propagate throughout the structure.

To summarize the convergence behavior of each integration approach (Gauss–Lobatto, Newton–Cotes, undetermined coefficients, and low-order undetermined coefficients) as the number of integration points increases, the error between the computed and exact solution is determined according to the definition

$$E(i) = \left| \frac{R(i) - R_{\text{exact}}(i)}{R_{\max}} \right| \cdot 100, \tag{15}$$

where i indicates a location ordinate as the load moves across the structure, R is the response ordinate, and $R_{\max}$ is the maximum response over all location ordinates in the exact solution. Scaling the absolute error by $R_{\max}$ rather than $R_{\text{exact}}(i)$ avoids spuriously large relative errors when the exact solution for the response ordinate is close to zero. The maximum percent error over all values of the location ordinate is shown in the bar charts in Figs. 7 and 8 for sections A and B, respectively. Each integration method gives identical results with $N = 3$, for which the well-known Simpson's rule is recovered in all cases. Gauss–Lobatto quadrature has the highest rate of convergence for increasing N, while the low-order approach converges at the slowest rate because the integration accuracy stays constant with increasing N. Newton–Cotes quadrature shows a reduction in the percent error up to $N = 9$, in which case a negative integration weight appears, causing the error to increase. There is a lack of convergence of the computed result to the exact solution with the method of undetermined coefficients for $N \geqslant 5$ due to the appearance of negative integration weights from the solution to Eq. (13) for the locations specified in Fig. 5.

5.2. Application to bridge analysis

The application of the low-order undetermined coefficients integration method in the force-based element formulation to computing the moment-shear demand history at critical sections in a structure is presented in this example for the moving load analysis of a conventionally reinforced concrete deck girder bridge. The structure is the McKenzie River Bridge, located on Interstate-5 just north of Eugene, OR, and shown schematically in Fig. 9. Each span is 15.25 m long and the girder is 1.22 m deep, and 0.33 m wide. Prismatic, linear-elastic response is assumed along each span using the elastic properties of concrete and the girder cross-section dimensions. A three-axle AASHTO HS-20 design truck [16] moves across the bridge.

A single force-based element is used to compute the response of each span, and the integration points for each element correspond to the seven span locations identified as critical for rating [17]. These critical locations, shown in Fig. 9, represent changes in stirrup spacing, flexural reinforcing steel cut-off

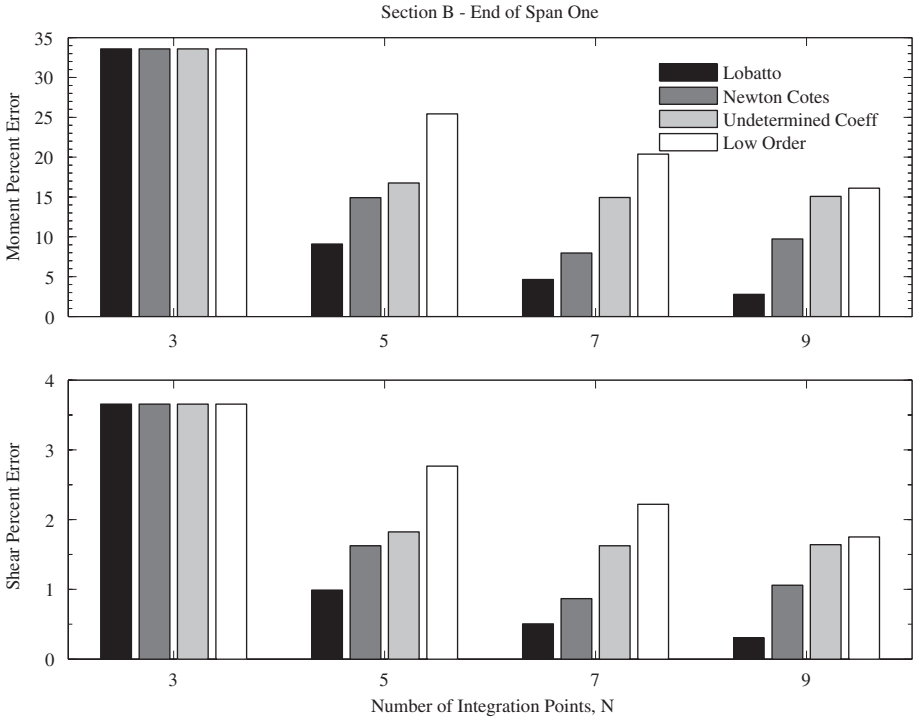

Fig. 8. Percent errors for the internal moment and shear computed at section B of the two-span structure in Fig. 4 for each numerical integration approach with an increasing number of integration points.

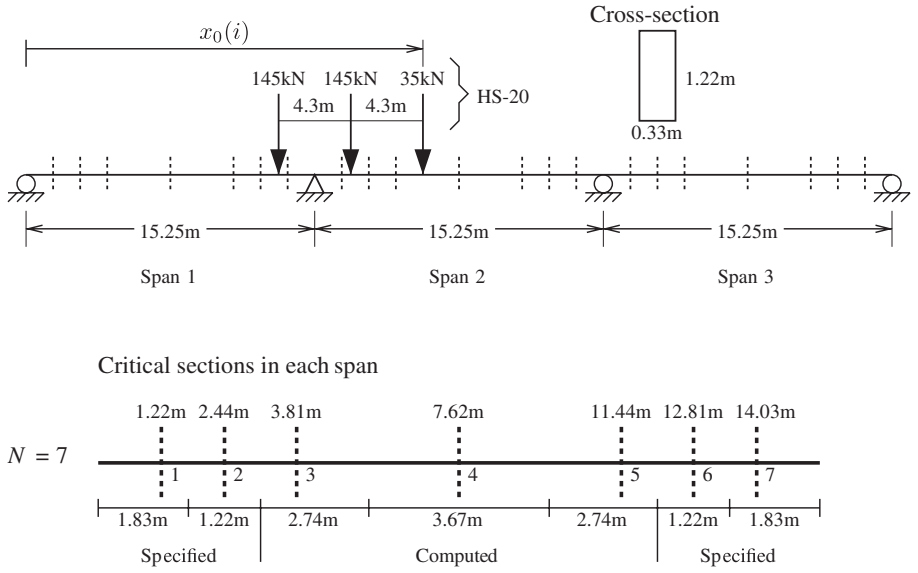

Fig. 9. Model of the McKenzie river bridge with seven section locations identified along each span as critical for rating.

locations, and locations of diagonal cracks from inspection data. To construct a quadrature method that uses these locations in the low-order approach to numerical integration, an integration weight of 1.83 m is assigned to sections 1 and 7, while a weight of 1.22 m (equal to the depth of the bridge girder) is assigned to sections 2 and 6. The remaining integration weights at sections 3–5 are determined by the solution of Eq. (14) to be approximately 2.74, 3.67, and 2.74 m, respectively.

The internal moment and shear demand history at each critical location due to the moving load pattern is computed using one force-based beam element in each span with the locations and weights of the integration points described above. The analysis results are shown in Fig. 10 for the moment and shear at the middle of span 1 and at the farthest right location (section 7) in span 2, 29.3 m from the left abutment. The computed moment and shear demand histories are very close to the exact

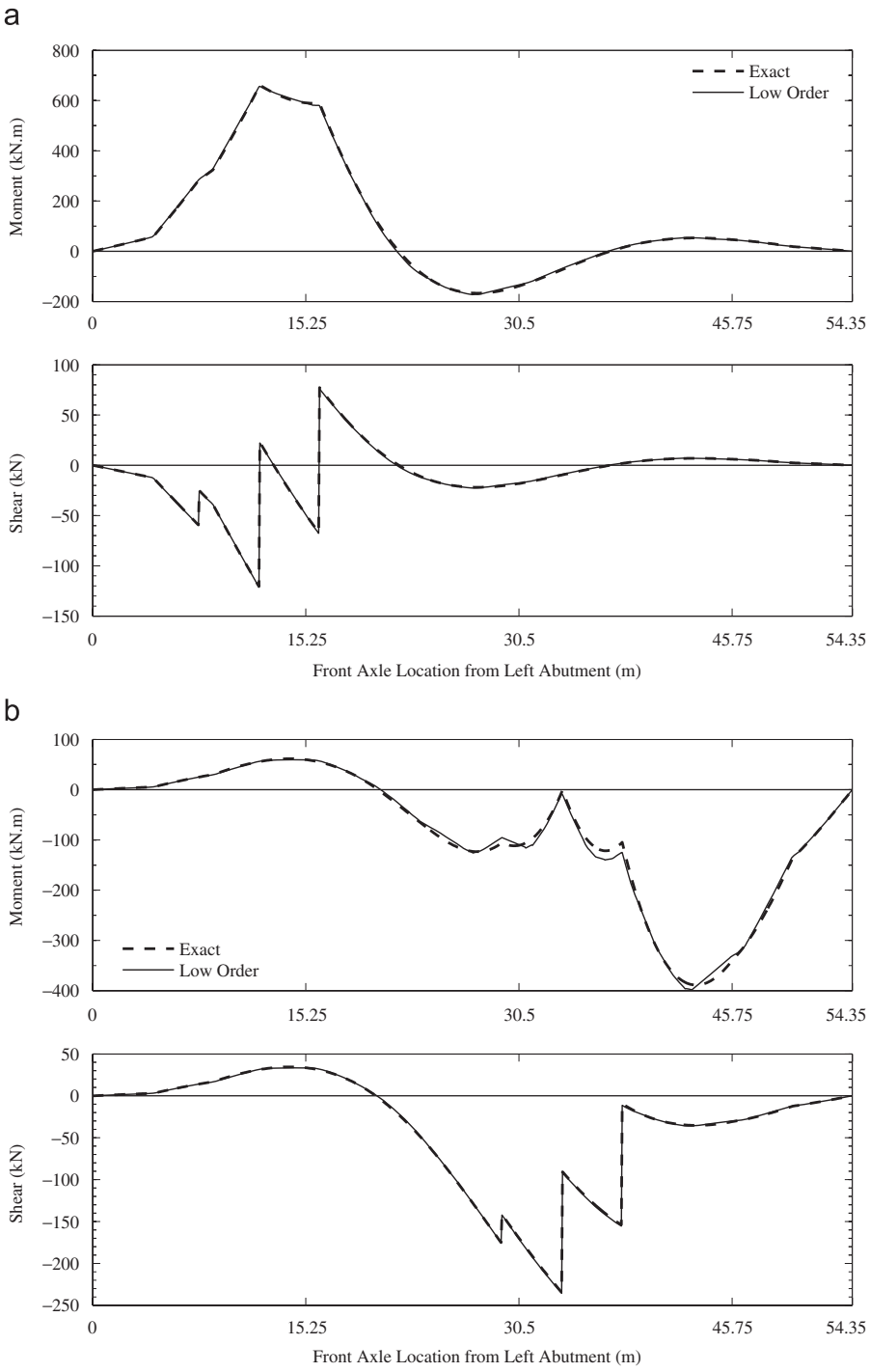

Fig. 10. Comparison between the computed and exact solution for the moment and shear demand histories at: (a) middle of span 1; and (b) span 2 at 29.3 m from the left abutment of the McKenzie river bridge.

solution, as shown in Fig. 10. The errors for the moment and shear at the middle of span 1 are 1.63% and 1.18%, respectively. Similarly, the errors for the moment and shear at 29.3 m from the left abutment are 4.93% and 0.785%, respectively. Considering the large amount of uncertainty in estimating structural capacity from design drawings, material properties, and field inspection data, this small difference between the computed and exact solution indicates that specifying critical sections as integration points within a force-based element using low-order integration is an accurate and reliable approach to computing the internal forces of a structure subjected to moving loads.

6. Conclusions

The advantages of using force-based finite elements in the moving load analysis of structures have been demonstrated. Since the force-based formulation imposes strong equilibrium between the section forces and the end moments and interior

element loads, only a single force-based finite element is required to simulate the response of a structural member to moving loads. Further discretization of the finite element model is not necessary, even as additional critical locations are included in the analysis. A new numerical integration approach was presented that allows the specification of critical locations in a structural member as the integration points of a force-based element. This integration approach maintains a low order of integration accuracy that is sufficient for practical applications in structural engineering. Accurate results for the moment and shear demand history at specified locations in a structure were obtained using force-based elements in conjunction with the new integration approach. Although the numerical examples focused on linear-elastic structural response, further applications of this integration approach include the representation, using a single force-based finite element, of the spread of plasticity across prescribed plastic hinge lengths and the smearing of moment–shear interaction over D-regions at continuous structural supports. The results of this research have been incorporated in load rating software developed for the Oregon Department of Transportation to rate the large number of bridges in the state inventory in an efficient manner [18].

Acknowledgments

This work was supported by the Oregon Department of Transportation under Grant no. MBMSFY04-041 awarded to Oregon State University. Their support is gratefully appreciated.

References

[1] T.J.R. Hughes, The Finite Element Method, Prentice-Hall, Englewood Cliffs, NJ, 1987.
[2] R.D. Cook, D.S. Malkus, M.E. Plesha, Concepts and Applications of Finite Element Analysis, third ed., Wiley, New York, NY, 1989.
[3] O.C. Zienkiewicz, R.L. Taylor, The Finite Element Method: The Basis, vol. 1, fifth ed., Butterworth, Stoneham, MA, 2000.
[4] E. Spacone, V. Ciampi, F.C. Filippou, Mixed formulation of nonlinear beam finite element, Comput. Struct. 58 (1996) 71–83.
[5] A. Neuenhofer, F.C. Filippou, Evaluation of nonlinear frame finite-element models, J. Struct. Eng. 123 (7) (1997) 958–966.
[6] G.H. Tan, G.H. Brameld, D.P. Thambiratnam, Development of an analytical model for treating bridge–vehicle interaction, Eng. Struct. 20 (1998) 54–61.
[7] S.-H. Ju, H.-T. Lin, C.-C. Hseuh, S.-L. Wang, A simple finite element model for vibration analyses induced by moving vehicles, Int. J. Numer. Methods Eng. 68 (2006) 1232–1256.
[8] L. Kwasniewski, H. Li, J.W. Wekezer, J. Malachowski, Finite element analysis of vehicle–bridge interaction, Finite Elem. Anal. Des. 42 (11) (2006) 950–959.
[9] F.C. Filippou, G.L. Fenves, Methods of analysis for earthquake-resistant structures. In: Y. Bozorgnia, V.V. Bertero (Eds.), Earthquake Engineering: From Engineering Seismology to Performance-based Engineering, CRC, Boca Raton, FL, 2004 (Chapter 6).
[10] G. Ranzo, M. Petrangeli, A fibre finite beam element with section shear modelling for seismic analysis of RC structures, J. Earthquake Eng. 2 (3) (1998) 443–473.
[11] J. Stoer, R. Bulirsch, Introduction to Numerical Analysis, second ed., Springer, New York, NY, 1993.
[12] M. Abramowitz, I.A. Stegun, Handbook of Mathematical Functions with Formulas, Graphs, and Mathematical Tables, 9th printing, Dover, New York, NY, 1972.
[13] M.H. Scott, G.L. Fenves, Plastic hinge integration methods for force-based beam-column elements, J. Struct. Eng. 132 (12) (2006).
[14] G.H. Golub, C.F. Van Loan, Matrix Computations, third ed., The Johns Hopkins University Press, Baltimore, MD, 1996.
[15] F. McKenna, G.L. Fenves, M.H. Scott, Open system for earthquake engineering simulation, ⟨http://opensees.berkeley.edu⟩, 2000.
[16] AASHTO. LRFD Bridge Design Specifications, second ed., American Association of State Highway and Transportation Officials, Washington, DC, 1998.
[17] C. Higgins, T.K. Daniels, D.V. Rosowsky, T.H. Miller, S.C. Yim, Reliability based assessment of conventionally reinforced concrete bridges for shear, J. Transp. Res. Board 1928 (2005) 110–117.
[18] M.H. Scott, C.C. Higgins, G. Esch, Reliability based bridge rating software. In: Seventh International Conference on Short and Medium Span Bridges, Montreal, Que, Canada, 2006, Paper #257.